



**HAL**  
open science

## Non thermal plasma in liquid media: Effect on inulin depolymerization and functionalization

Raluca Nastase, Elodie Fourre, Mathieu Fanuel, Xavier Falourd, Isabelle Capron

► **To cite this version:**

Raluca Nastase, Elodie Fourre, Mathieu Fanuel, Xavier Falourd, Isabelle Capron. Non thermal plasma in liquid media: Effect on inulin depolymerization and functionalization. Carbohydrate Polymers, 2020, 231, pp.115704. 10.1016/j.carbpol.2019.115704 . hal-02944380

**HAL Id: hal-02944380**

**<https://hal.inrae.fr/hal-02944380v1>**

Submitted on 27 Nov 2020

**HAL** is a multi-disciplinary open access archive for the deposit and dissemination of scientific research documents, whether they are published or not. The documents may come from teaching and research institutions in France or abroad, or from public or private research centers.

L'archive ouverte pluridisciplinaire **HAL**, est destinée au dépôt et à la diffusion de documents scientifiques de niveau recherche, publiés ou non, émanant des établissements d'enseignement et de recherche français ou étrangers, des laboratoires publics ou privés.



Distributed under a Creative Commons Attribution - NonCommercial - NoDerivatives 4.0 International License

# 1 **Non thermal plasma in liquid media: effect on inulin depolymerization and** 2 **functionalization**

3 Raluca Nastase<sup>1,2</sup>, Elodie Fourré<sup>1</sup>, Mathieu Fanuel<sup>2</sup>, Xavier Falourd<sup>2</sup>, Isabelle Capron<sup>2</sup>

4 <sup>1</sup>*Research unit on catalysis and unconventional media, IC2MP, Poitiers, France*

5 <sup>2</sup>*UR1268 Research unit Biopolymers, interactions and assemblies (BIA), INRA, Nantes, France*

6 *Corresponding author: elodie.fourre@univ-poitiers.fr*

## 7 Keywords

8 Gas-liquid plasma reactor; non thermal plasma; inulin; depolymerization; infrared  
9 spectroscopy; ssNMR spectroscopy

## 10 Highlights

- 11 • A novel double dielectric barrier discharge plasma reactor with a liquid interface has  
12 been designed
- 13 • It is possible to totally convert inulin into 100 % fructose and glucose
- 14 • No degradation products are generated
- 15 • Combined analytical results evidenced the acidic attack of the glycosidic bond leading  
16 to depolymerization

## 17 Abstract

18 We report the complete conversion of inulin in gas/liquid media by a dielectric barrier discharge  
19 plasma at atmospheric pressure. Depending on the plasma treatment time (from 1 to 30 min)  
20 and the chemical nature of the gases (air, oxygen, nitrogen), it was possible to depolymerize  
21 inulin into fructo-oligosaccharides with a degree of polymerization inferior to 5 or to achieve a  
22 total conversion of inulin into its two monomeric constituents, fructose and glucose in 20 min,  
23 without any degradation products. Combined results from liquid chromatography (HPLC),  
24 solid state Nuclear Magnetic Resonance (ssNMR) and mass spectroscopy revealed that the  
25 breakage of the  $\beta$  1-4-bridged oxygen occurs by an acidic attack, following the oxidation of the

26 polymer. Infrared spectroscopy revealed the oxidation and breakage of the polymer and also  
27 adsorption of nitrate species.

## 28 Introduction

29 Since the industrial revolution, chemistry has developed processes, catalysts and technologies  
30 for the conversion of fossil carbon, aiming to create complex and diverse molecules. However,  
31 increasing environmental awareness is prompting scientists and manufacturers to develop  
32 strategies for environmental sustainability by using processes and materials with low cost, low  
33 energy consumption and low toxicity. For several years now, a new approach has been focusing  
34 on the use of new raw material from the biomass or waste (Ong et al., 2019; Sheldon, 2018).  
35 This change of strategy was revolutionary in the world of chemistry and it has dramatically  
36 changed the way a process is designed (Jérôme, Chatel & De Oliveira Vigier, 2016; Farmer &  
37 Mascal, 2015; Sylla-Iyarreta Veitía & Ferroud, 2015; Horváth & Anastas, 2007; Baig & Varma,  
38 2012; Benoit et al., 2012). For this reason, the use of advanced technologies, such as non-  
39 thermal plasma, ultrasounds or ball-milling have been extensively investigated (Farmer &  
40 Mascal, 2015). Current and future society needs scientists and manufacturers to focus on new  
41 strategies and develop low cost processes for sustainable materials, easy to produce and widely  
42 available (Jérôme, 2016)

43 The recent extensive use of non-thermal plasma is the result of a range of reaction parameters  
44 that cannot be accessible otherwise, or to a lesser extent. No other media can provide gas  
45 temperatures or energy densities as high as those of plasmas; no other media can excite atomic  
46 and molecular species to radiate as efficiently; no other media can be arranged to provide  
47 comparable transient and non-equilibrium conditions (National Research Council, 1991). This  
48 technology is safe, versatile, easy to carry out and allows the generation of highly reactive  
49 chemical species with low energy consumption, low toxicity and the possibility of continuous  
50 processing (Kan, Lam, Chan, & Ng, 2014).

51 The development of atmospheric pressure plasma technologies has dramatically increased in  
52 recent years due to their potential impact in a very wide range of applications that include  
53 surface treatments (cleaning, etching), surface activation, surface coating (air plasma spray,  
54 plasma enhanced chemical vapor deposition) (Tendero, Tixier, Tristant, Desmaison &  
55 Leprince, 2006), but also food (decontamination, toxin degradation, packaging), medicine  
56 (sterilization, wound healing, skin treatments) and water (pesticide and dyes degradation,  
57 decontamination) (Pankaj & Keener, 2017). The technological progress has encouraged the  
58 interest and advancement in the understanding of plasmas. The possibility of performing  
59 reactions at atmospheric pressure is becoming increasingly attractive and the fundamental and  
60 essential role of technological plasmas is set to expand significantly in the coming years  
61 (Mariotti, Patel, Švrček & Maguire, 2012).

62 In this context, production of fructose from fructans such as inulin using plasma, is an  
63 alternative to the current approaches, such as acid or enzymatic hydrolysis (Raccuia et al.,  
64 2016). Inulin is constituted of fructose units connected by  $\beta$  (1-2) linkages with a glucose at its  
65 extremity linked in  $\alpha$  (1-2) form. In the inulin chain, the fructose is blocked in the furanose form  
66 and glucose is in glucopyranose form. Inulin, its derivatives and its two constitutive monomers  
67 have received considerable interest as food ingredients (Blecker, Fougny, Van Herck,  
68 Chevalier & Paquot, 2002). Inulin has also been chemically modified in several ways (neutral,  
69 anionic, and cationic modification as well as cross-linking and slow release applications) to  
70 obtain highly biodegradable compounds at the industrial scale (Stevens, Meriggi & Booten,  
71 2001).

72 The effect of non-thermal atmospheric plasma on inulin was already investigated on solid  
73 material in gas phase but the reaction mechanism was not completely elucidated [Nastase,  
74 Tatibouët & Fourré, 2018; Benoit & al., 2012). The authors reported the depolymerization of  
75 inulin with a yield of 16 wt % of fructose (other products being fructo-oligosaccharides (FOS)

76 with a degree of polymerization (DP) lower than 6) via the surrounding water initially contained  
77 in polysaccharides that promotes the cleavage of the glycosidic bonds (Benoit & al.). In a recent  
78 study (Nastase, Tatibouët & Fourré, 2018), it was suggested that reactive oxidizing species  
79 generated by oxygen (ROS) and nitrogen (RNS) played a key role in the depolymerization  
80 process, via OH radicals or nitric acid attack.

81 Nowadays, within the field of plasma science and technology, the attention is increasing over  
82 the plasma-liquid interactions, and particularly on the physical and chemical mechanisms  
83 leading to complex reaction at the plasma-liquid interface (Bruggeman et al, 2016). It is well  
84 admitted in the literature that discharges generated at the gas-liquid interface provide gaseous  
85 reactive species that can dissolve in the liquid media, inducing the formation of species  
86 presenting high reactivity, such as  $\text{H}_2\text{O}_2$ ,  $\text{NO}_2^- / \text{NO}_3^-$ ,  $\text{OH}^\bullet$ ,  $\text{HOO}^\bullet / \text{O}_2^{\bullet-}$  to name a few. The  
87 fundamental properties of liquid-phase plasma (like generation, state or reactive species) have  
88 not been fully described, but the presence of liquid in the system leads to higher reaction rate  
89 since the molecular density in the liquid phase is much higher than in the gas phase (Takai,  
90 2008). However, plasmas in liquids are more difficult to control and stabilize: the liquid is often  
91 an electrode, therefore evaporation and chemical modification occurs, which adds significant  
92 complexity compared to the gas phase plasmas (Bruggeman & Leys, 2009).

93 In this respect, a reactor with a double dielectric (DD) barrier, combining a liquid and gas phase  
94 DD-LG plasma has been developed. The configuration of the reactor used along this study  
95 allows the initiation of various types of reactions: plasma active species formed in the gas and  
96 at the gas-liquid interface are further transferred into the liquid giving rise to more chemical  
97 reactions. The novelty of this configuration resides in the isolation of the liquid phase between  
98 the 2 electrodes, which can avoid problems like electrode evaporation (when using liquid  
99 electrode) or contamination from the metal electrode in contact with the liquid. This plasma  
100 configuration has been used to follow depolymerization of inulin into FOS, fructose and glucose

101 investigated in controlled conditions in power, time, chemical nature of the gas phase and  
102 sample concentration.

## 103 1. Experimental

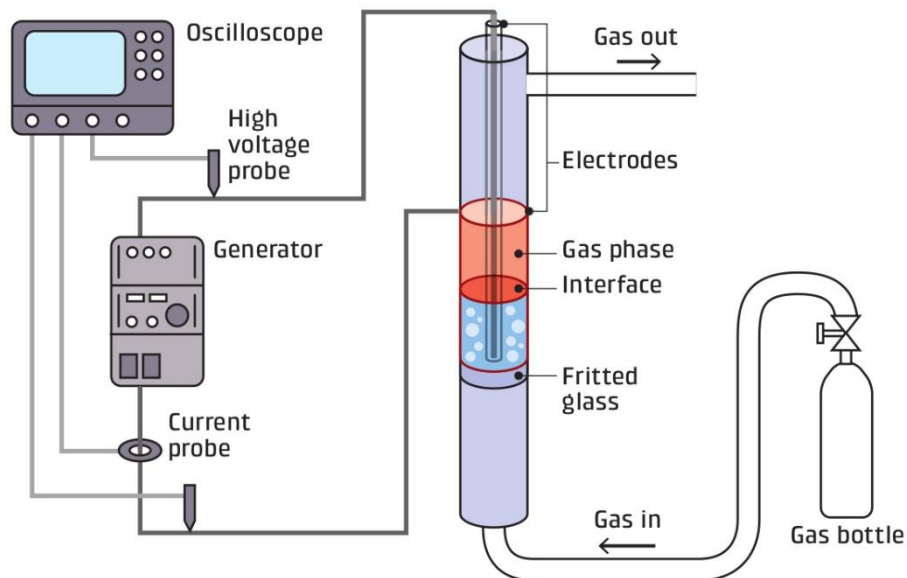
### 104 1.1. Materials

105  
106 Throughout this study, commercial inulin (from chicory, Sigma Aldrich) was used as a  
107 substrate. Inulin was solubilized in ultra-pure water under stirring at room temperature, to  
108 obtain a concentration of 8 g.L<sup>-1</sup> without further treatment.

### 109 1.2. Gas-liquid plasma device

110  
111  
112 Plasma treatment was carried out in a dielectric barrier discharge reactor consisting in a double  
113 wall glass cylinder separated in two parts by a fritted glass (figure 1). This reactor can be  
114 classified as multiphase discharge (Bruggeman et al., 2016) except that both electrodes are  
115 isolated from the liquid phase by two glass walls. The first electrode (inox tube) stands in the  
116 center of the cylinder and was protected from the liquid by a first dielectric wall. The second  
117 electrode (copper adhesive tape, from Advance tape) was wrapped around the second dielectric  
118 wall, on the outside wall of the cylinder. The gap between both dielectrics was 3 mm. A high  
119 voltage supply (A2E Technologies Enertronic), was connected to the electrodes and providing  
120 bipolar voltage pulses, allows the variation of the voltage from 0 to 40 kV. The gas (flow of 30  
121 mL.min<sup>-1</sup>) was introduced in the reactor from the bottom entry and was flown through a fritted  
122 glass which not only created bubbles, but also prevented the liquid from draining. The volume  
123 of the solution to be treated was set at 5 mL, allowing the generation of plasma in the gas phase,  
124 right above the surface of the liquid and, in a lesser extent, in the gas bubbles through the liquid.  
125 The solution was injected in the system kept at atmospheric pressure, room temperature and  
126 with the gas flow set at 30 mL min<sup>-1</sup>. In order to determine the optimal parameters for inulin  
127 conversion, the electrical parameters (voltage, 16-21 kV) and the treatment time (1-40 min)

128 were modified. The discharge was generated under nitrogen, oxygen, helium and air  
129 atmosphere



130

131 Figure 1: Drawing of the experimental setup

132

### 133 1.3.Characterization

#### 134 *Hydrogen peroxide content*

135

136 Hydrogen peroxide produced during the plasma treatment was calculated from colorimetric  
137 titration with potassium permanganate, in acidic conditions. 10 mL of plasma treated sample  
138 was placed in a beaker with 20 mL distilled water and 10 mL of H<sub>2</sub>SO<sub>4</sub> solution (3 M). The  
139 solution was magnetically stirred and a solution of KMnO<sub>4</sub> (0.025 M) was added dropwise  
140 through a graduated burette. The concentration was calculated from the equivalent point  
141 volume.

#### 142 *HPLC*

143 High Pressure Liquid Chromatography was used to determine the presence of oligosaccharides  
144 after plasma processing. Samples were analyzed on a Shodex Sugar KS-802 column  
145 (maintained at 40°C) that allows the separation of oligosaccharides by steric exclusion and

146 ligand exchange. The stationary phase consists of polystyrene-divinylbenzene coated with a  
147 cation exchange resin and the mobile phase consists of ultra-pure water at a flow rate of 1  
148 mL.min<sup>-1</sup>.

149 Molecules were eluted depending on their hydrodynamic volume. The concentrations of  
150 fructose and glucose were defined for each compound by a calibration curve established with  
151 different concentrations (supplementary information), giving the concentration in g.L<sup>-1</sup> of the  
152 analyzed compound as a function of the area of the chromatographic peaks.

### 153 *Solid state Nuclear Magnetic Resonance*

154 Solid state <sup>13</sup>C NMR experiments were carried out using a Bruker Avance III 400 MHz  
155 spectrometer operating at a <sup>13</sup>C frequency of 100.62MHz and equipped with a CP/MAS 4 mm  
156 <sup>1</sup>H/<sup>13</sup>C probe. Prior to the analysis, the samples were neutralized with a solution of NaOH (0.1  
157 M) and lyophilized. The pH was measured with a pHmeter (Eutech instrument pH510). The  
158 solid samples were packed in a 4 mm NMR rotor without any other preparation. The sample  
159 were spun at a rate of 9 kHz at room temperature. The cross polarization pulse sequence  
160 parameters were as follow : 3.95 μs for proton 90° pulse, a contact time between 0.8 and 2.0  
161 ms and 10 s recycle time. Usually, the accumulation of 5120 scans was used. The carbonyl  
162 signal of glycine (176.03 ppm) was used to calibrate the chemical shift of the <sup>13</sup>C NMR spectra.  
163 The chemical shift, peak half-width and peak area of the different peaks were determined with  
164 a least squares fitting method using Peakfit® software

### 165 *Mass spectrometry*

166  
167 The samples analyzed by ssNMR were also analyzed by matrix-assisted laser  
168 desorption/ionization (MALDI)-time-of-flight (TOF) MS. For the measurements, an ionic  
169 preparation of 2,5-dihydroxybenzoic acid (DHB) and N,N-dimethylaniline (DMA) was used as  
170 the MALDI matrix, as described in (Ropartz, 2011). Briefly, the matrix consists of a mixture



171 of DHB and DMA (DHB 100 mg.ml<sup>-1</sup>, in H<sub>2</sub>O/acetonitrile/ DMA (1:1:0.02)) and was mixed  
172 with the samples in a 1:1 ratio (v/v). The mixture (1 μL) was then deposited on a polished steel  
173 MALDI target plate. MALDI measurements were then performed on an Autoflex Speed  
174 MALDI-TOF/TOF spectrometer (Bruker Daltonics, Bremen, Germany) equipped with a  
175 Smartbeam laser (355 nm, 1000 Hz) and controlled using the Flex Control 3.0 software  
176 package. The mass spectrometer was operated with positive polarity in reflectron mode. Spectra  
177 were acquired in the range of 180–3500 *m/z*.

178 The evolution of the percentage of DP 1 was then monitored using the following formula:

179 
$$\% = \frac{I_{DP1}}{I_{DP1}+I_{DP2}+I_{DP3}+I_{DP4}} \quad \text{equation 1}$$

## 180 *FT-IR*

181 Fourier transform infrared spectroscopy was performed before and after plasma treatment in  
182 order to observe the eventual functionalization and/or stabilization of species on the surface of  
183 inulin. Prior to analysis, the sample was lyophilized. The powder sample (5 mg) was mixed  
184 with KBr (100 mg) and pressed in a hydraulic press and then recovered in the form of a pellet.  
185 The analysis was carried out in a Nicolet IS50 spectrometer in transmission mode and the  
186 resulting spectra were an average of 200 scans at a resolution of 16 cm<sup>-1</sup>. All spectra were  
187 baseline corrected and normalized to be compared to each other.

## 188 2. Results and discussion

### 189 2.1. Reactor optimization

190

191 In order to identify the reactivity sites (in gas bubbles, in the upper gas phase or at liquid-gas  
192 interface) and to evaluate the discharge propagation, the effect of the volume of liquid submitted  
193 to plasma was studied, introducing 5 mL, 10 mL and 15 mL of an aqueous solution of inulin at  
194 8 g.L<sup>-1</sup> (figure 2). The experiments were carried out at constant voltage (19 kV), frequency (2  
195 kHz) and time (20 min). The efficiency of the plasma discharge was evaluated by its impact on

196 inulin depolymerization via the following of fructose yields, pH, and  $\text{NO}_2^- / \text{NO}_3^-$  and  $\text{H}_2\text{O}_2$   
197 concentrations.

198 When 15 mL were introduced, the inulin solution filled the reactor with 5 mL of the volume  
199 standing above the external electrode limit. No depolymerization occurred in this configuration.  
200 Additionally, no pH change was observed and no other species were detected (Table 1). It  
201 appeared that the observed discharge was occurring in the tube holding the central electrode, as  
202 a very small air gap was present between the electrode and the inner wall of the dielectric barrier  
203 (visible on figure 1). When the inner tube was sealed with glue, no plasma discharge was  
204 observed, neither depolymerization.

205 When 10 mL of solution were inserted in the reactor, it allowed the development of the plasma  
206 at the gas-liquid interface but without (or very little) plasma in the gas phase. A concentration  
207 of only  $0.14 \text{ g.L}^{-1}$  of fructose was detected and, in the same time, pH dropped from 6.5  
208 (untreated solution) to 5.0. Using semi quantitative test strips (Quantofix), a small fraction of  
209  $\text{NO}_x^-$  species were measured indicating the dissolution of nitrous oxides into nitrites ( $1 \text{ mg.mL}^{-1}$ )  
210 and nitrates ( $\leq 10 \text{ mg.mL}^{-1}$ ).

211 Finally, 5 mL of solution introduced resulted in a system with two phases of plasma, at interface  
212 and in the gas phase. In this case, inulin was totally depolymerized into fructose ( $7 \text{ g.L}^{-1}$ ),  
213 glucose ( $0.25 \text{ g.L}^{-1}$ ) and a compound of DP 2. It clearly showed that the most effective reaction  
214 occurred when the gas-liquid interface and even more importantly, the plasma in gas phase are  
215 present. From these results, the configuration using 5 mL of solution was kept throughout the  
216 study.

217 The fact that the depolymerization was enhanced in presence of a gas phase highlighted the fact  
218 that the long lived plasma species from the gas phase may be responsible of the reactivity. Their  
219 dissolution in the liquid media would lead to active species capable to dissociate the polymer.

220 In order to verify this hypothesis the reactor was turned upside down, allowing only the contact  
 221 of the plasma long lived species with the liquid. It resulted in no modification of the inulin  
 222 chain. The pH of the solution decreased to 3.4, indicating the dissolution of acidic species from  
 223 the gas phase in the liquid, but no depolymerization occurred. It has been established in the  
 224 literature (Bruggeman et al., 2016; Takai, 2008) that the active species generated in the gas  
 225 phase are transferred from the gas to the liquid phase, creating more reactive species such as  
 226 H<sub>2</sub>O<sub>2</sub>, peroxonitrites (ONOO<sup>-</sup>) and nitric acid (HNO<sub>3</sub>). Among the species commonly produced  
 227 in the liquid phase, H<sub>2</sub>O<sub>2</sub>, NO<sub>2</sub><sup>-</sup> and NO<sub>3</sub><sup>-</sup> were detected in the samples after plasma treatment  
 228 (Table 1). In the case of air treatment, NO<sub>3</sub><sup>-</sup> was detected up to 500 mg.mL<sup>-1</sup>.

229 Table 1: pH, NO<sub>2</sub><sup>-</sup> / NO<sub>3</sub><sup>-</sup> and H<sub>2</sub>O<sub>2</sub> concentrations measured after 20 min of air plasma treatment  
 230 for different liquid volumes. Parameters: P = 28 W, gas flow = 30 mL.min<sup>-1</sup>, f = 2 kHz; [inulin]  
 231 = 8 g.L<sup>-1</sup>

Volume	15 ml	10 ml	5 ml	Upside down (5 mL)
pH	6.5	5	1.5	3.4
H <sub>2</sub> O <sub>2</sub> mg.mL <sup>-1</sup>	0	10	11.2	1.5
NO <sub>2</sub> <sup>-</sup> mg.mL <sup>-1</sup>	0	1	15	0
NO <sub>3</sub> <sup>-</sup> mg.mL <sup>-1</sup>	0	15	500	350

232

## 233 2.2. Varying the chemical nature of the plasma gas

234

235 In order to further identify and evaluate the reactivity of plasma chemical active species in such  
 236 a system, the depolymerization reaction of inulin was performed using different gases. The  
 237 results are summarized in table 2. The highest concentration of H<sub>2</sub>O<sub>2</sub> was measured under  
 238 oxygen and O<sub>2</sub>/He plasma. Under nitrogen and air plasma the H<sub>2</sub>O<sub>2</sub> concentrations were lower,  
 239 due to the presence of NO<sub>2</sub><sup>-</sup>, which in acidic conditions can lead to the H<sub>2</sub>O<sub>2</sub> degradation

240 (Gorbanev, O'Connell & Chechik, 2016; Lukes, Dolezalova, Sisrova & Clupek, 2014). The  
 241 lowest concentration was measured under pure helium plasma.

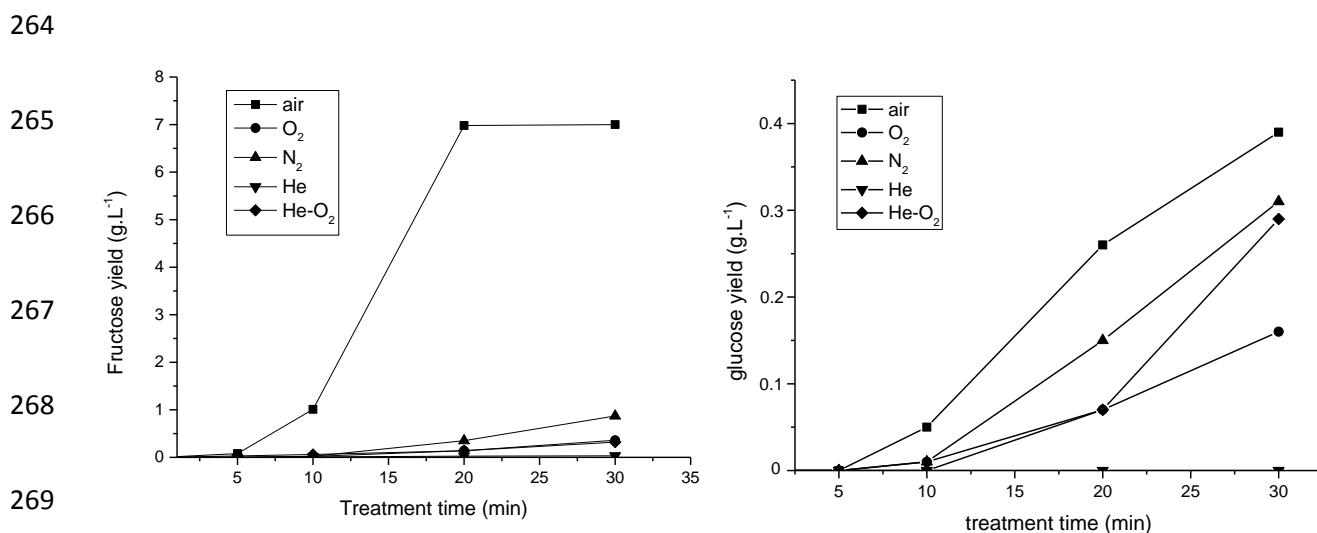
242 Table 2: fructose concentration, pH and oxidized species concentrations measured after 20 min  
 243 of plasma treatment for different gas phases. Parameters: gas flow = 30mL.min<sup>-1</sup>, f = 2 kHz;  
 244 [inulin] = 8 g.L<sup>-1</sup>

Gas nature	100 % O <sub>2</sub>	100 % He	50% He / 50% O <sub>2</sub>	100 % N <sub>2</sub>	Synthetic air
Power (W)	12	12	28	14	28
Fructose conc. (g.L <sup>-1</sup> )	0.3	0.02	0.3	0.9	7
pH	3-4	3-4	3-4	1.5	1.5
H <sub>2</sub> O <sub>2</sub> (mmol.L <sup>-1</sup> )	15.5	3.6	13.7	10	11.2
NO <sub>3</sub> <sup>-</sup> (mg.L <sup>-1</sup> )	none	none	none	250 ≥ x ≥ 500	≥ 500
NO <sub>2</sub> <sup>-</sup> (mg.L <sup>-1</sup> )	none	none	none	5 < x < 10	15

245  
 246 The fructose concentration measured after plasma treatment under helium was the lowest (0.02  
 247 g.L<sup>-1</sup>). The actives species generated under helium plasma such as He<sup>\*</sup>, He<sub>2</sub><sup>\*</sup>, He<sup>+</sup> and He<sub>2</sub><sup>+</sup>, but  
 248 also dissolved oxygenated species generated from electron and helium impact on water  
 249 molecules, are not participating in the reaction in the first 30 min. Oxygen gas appeared also  
 250 quite inert since the addition of oxygen to helium gas and higher injected power in the reactor  
 251 did not affect the fructose yield as compared with pure oxygen (0.3 g.L<sup>-1</sup>). When pure nitrogen  
 252 was flown through the system, a slight increase of fructose concentration was observed but to  
 253 a lesser extent compared to air treatment where inulin was totally converted. It is worth  
 254 mentioning that an air plasma treatment at 12W resulted in no conversion.

255 The HPLC results of the plasma treatment under synthetic air showed the progressive  
 256 depolymerization of inulin into smaller fractions and its two constituents, glucose and fructose.  
 257 Air plasma is the most effective treatment for the inulin depolymerization. A treatment time of  
 258 approximately 20 min allowed the total conversion of inulin (figure 2). The concentration of  
 259 fructose was 7 g.L<sup>-1</sup> reaching a plateau at 20 and 30 min. Interestingly, the glucose concentration

260 (figure 2b) increased until 30 min of treatment ( $0.4 \text{ g.L}^{-1}$ ). It appears that the reactive species  
 261 derived from the reactions between nitrogen and oxygen in the air plasma are responsible for  
 262 the depolymerization. Nitrous oxides solvation in water would lead to nitric and nitrous acids,  
 263 providing  $\text{H}^+$  ions and consequently acid hydrolysis of the polymer.



270 Figure 2: plot of a) fructose and b) glucose yields as a function of treatment time. Conditions: 2 kHz, 30  
 271  $\text{mL.min}^{-1}$ ; P = 28 W and P (He) = 12 W; [inulin] =  $8 \text{ g.L}^{-1}$

272

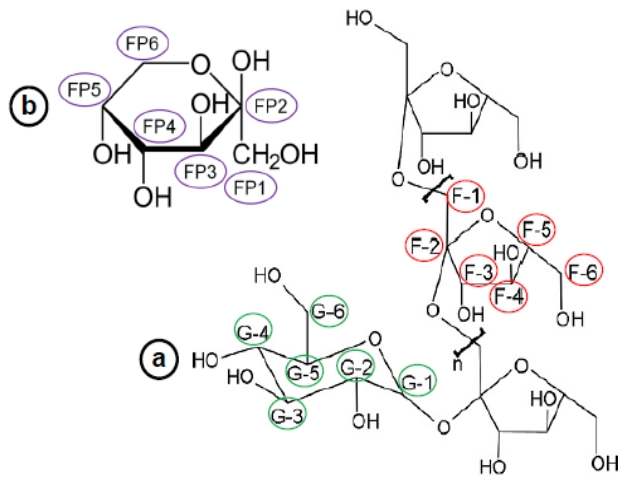
273 A series of tests with nitric acid were performed in order to confirm this hypothesis. When 5ml  
 274 of inulin solution were mixed with nitric acid ( $1 \text{ mol.L}^{-1}$ ) till a pH = 1.5, followed by  $80^\circ\text{C}$   
 275 heating from 20 to 100 min, a total conversion into fructose ( $8\text{mg.ml}^{-1}$ ) was achieved. The same  
 276 result was obtained when inulin powder was added to plasma treated water (in air; P = 28 W)  
 277 and heated up at  $80^\circ\text{C}$ . The pH of the water treated with air plasma equaled 1.5. These  
 278 experiments confirmed the participation of  $\text{H}^+$  in the depolymerization process.

### 279 2.3.Elucidating the depolymerization process

280

281  $^{13}\text{C}$  CP/MAS NMR spectroscopy was used for anomer analyses of reducing terminal units of  
 282 the treated chains in order to follow depolymerization under air plasma treatment, which proved  
 283 to be the most efficient treatment. A freeze dried reference (no plasma) was prepared and  
 284 compared to samples treated in air up to 20 min. The structure of inulin (a), along with the  $\beta$ -

285 D-fructopyranose form (b) detected in some samples is represented in figure 6. When  
 286 glucopyranose is present at the reducing end, the fructose molecules are in the furanose form.  
 287 Without glucose at the end, the fructose molecules are in the pyranose form (Levy & Fügedi,  
 288 2005). The labelling on the NMR spectra are also referenced in figure 3.



289  
 290 Figure 3: Structure of a) inulin and b)  $\beta$ -D-fructopyranose

291  
 292 After spectral deconvolution, the average degrees of polymerization have been calculated using  
 293 the next formula:

294 For untreated inulin, the lyophilized untreated inulin and inulin treated by plasma for 3 min:

$$295 \quad DP \text{ average} = \frac{\left[ \frac{\sum \text{area from 83 to 57 ppm}}{5} \right] - \text{area at 93 ppm}}{\text{area at 93 ppm}} \quad \text{Equation 2}$$

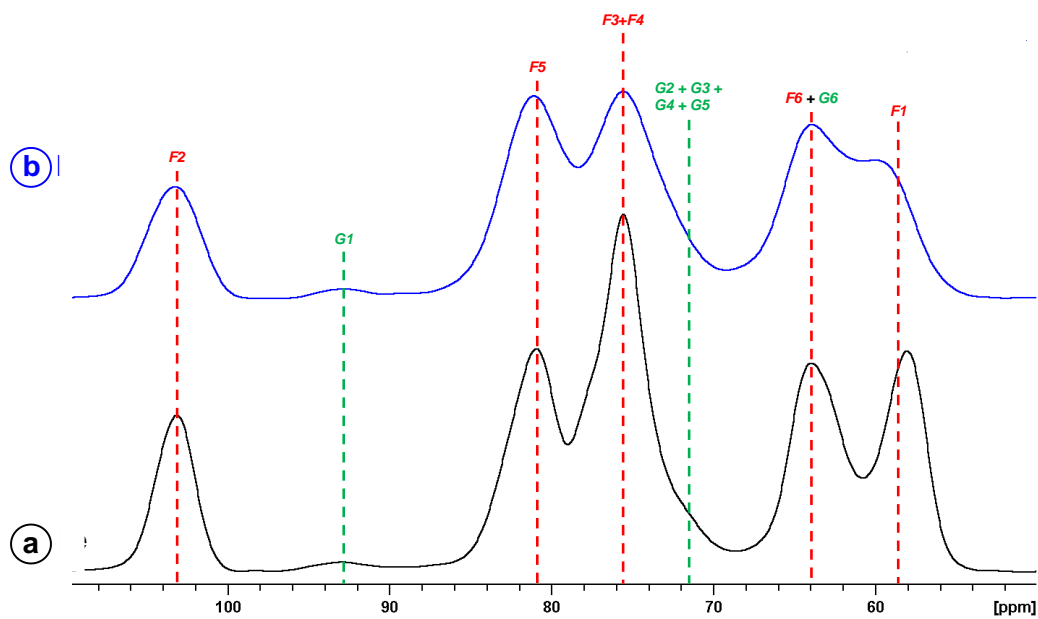
296 The numerator corresponds to the signal of fructose monomers subtracted from glucose  
 297 contribution (figure 4). The denominator corresponds to the signal of anomeric carbons of  
 298 ending glucose.

299 Inulin treated by plasma from 7 to 40 min:

$$300 \quad DP \text{ average} = \frac{[(\sum \text{area from 83 to 57 ppm})/5] - (\text{area at 93 ppm} + \text{area at 98 ppm})}{(\text{area at 93 ppm} + \text{area at 98 ppm})} \quad \text{Equation 3}$$

301 The peak at 93 ppm corresponds to the glucose reducing end in the  $\alpha$  conformation and the  
302 peak at 98 ppm in the  $\beta$  conformation or C<sub>2</sub> from fructopyranose (Colombo, Aupic, Lewis &  
303 Mario Pinto, 2015).

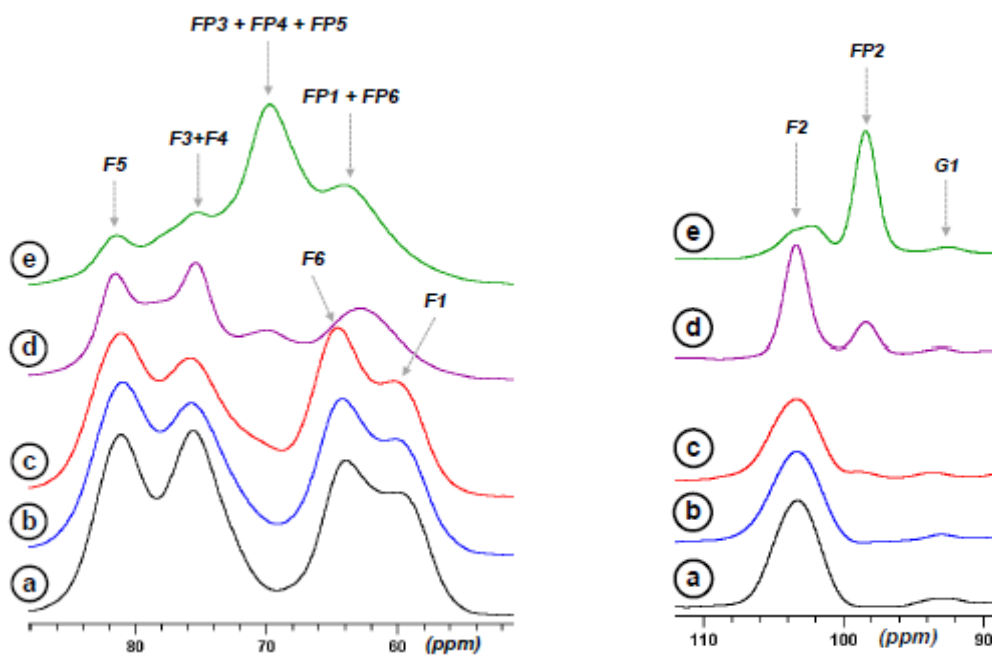
304 The NMR analysis of the freeze dried reference (figure 4) highlighted the presence of  
305 fructopyranose form of inulin and showed that the freeze-drying step was also affecting the  
306 supramolecular organization of inulin. The widening of the bands at 103 ppm and in both  
307 regions 86-70 ppm and 68-54 ppm reflected a less ordered structure after lyophilization, most  
308 probably arising from a loss of the crystallinity. In addition, the chemical shift of C<sub>1</sub> (F1) of  
309 fructose, between 80 and 74 ppm, was modified suggesting a significant change of the magnetic  
310 environment.



311

312 Figure 4: <sup>13</sup>C CP/MAS inulin spectra, (a) initial state, (b) after solubilization and lyophilization.  
313 (Annotations are referring to figure 3).

314



315

316 Figure 5:  $^{13}\text{C}$  CP/MAS spectra zones of non-anomeric carbons (left panel) and anomeric carbon (right  
 317 panel) of (a) lyophilized inulin (reference) and after plasma treatment of (b) 3 min, (c) 7 min,  
 318 (e) 20 min. (Annotations are referring to figure 6)

319

320 Figure 5 shows the  $^{13}\text{C}$  CP/MAS spectra of inulin before and after up to 20 min of plasma  
 321 treatment. As the time of plasma treatment increased, peaks in the 110 – 90 ppm and 90 – 55  
 322 ppm regions evolved differently. The anomeric and non-anomeric carbon peaks of furanose  
 323 ring, labelled F1 to F6, are decreasing as the treatment time increases. At 7 min of treatment,  
 324 an anomeric carbon (FP2) presenting a chemical shift at 98.4 ppm is emerging, identified as C<sub>2</sub>  
 325 carbons of free fructose in the  $\beta$ -D-fructopyranose form (Colombo, Aupic, Lewis & Mario  
 326 Pinto, 2015; Shiomi & Onodera, 1990). The proportion of this signal increases with treatment  
 327 time. The presence of free  $\beta$ -D-fructopyranose is confirmed by peaks in the non-anomeric  
 328 carbon region at 70 ppm and 84 ppm, which increases as a function of treatment time. It is  
 329 worth mentioning that the pyranose form of fructose was predominant during the solubilization  
 330 step of monomeric fructose. This result indicates that the conversion from the furanose to



331 pyranose form is most likely to occur during the neutralization step and is not due to the plasma  
332 treatment.

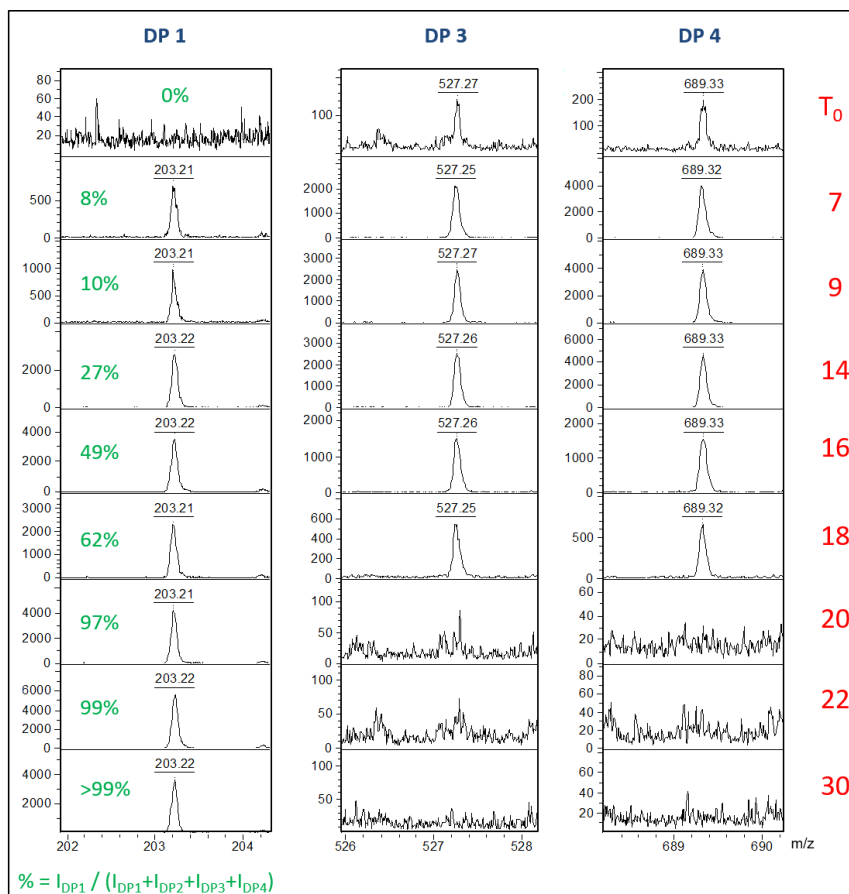
333 From equations (2) and (3), average values of the degrees of polymerization were calculated  
334 (table 3). It shows that after 3 min, a clear depolymerization occurs as already shown by the  
335 HPLC. A progressive decrease of the DP was observed as a function of the plasma treatment  
336 time up to monomers, without further degradation.

337 Table 3: Calculated average degree of polymerization (DP) of air plasma treated inulin: P = 28 W; f = 2  
338 kHz; flow rate: 30 mL.min<sup>-1</sup>

	DP
Commercial inulin	30
Lyophilized inulin	29
3min	27
7min	13
13min	3
20min	1

339

340 To investigate the molecular polydispersity of the released products and more specifically the  
341 proportion of DP 1 throughout the treatment of inulin by the plasma, MALDI-TOF MS analyses  
342 were performed (figure 6). The evolution of the proportion of DP 1 compared to DP 2, 3 and 4  
343 was monitored by mass spectrometry, using the equation 1. These experiments showed that  
344 above 20 min, it remains almost only DP 1 species (glucose and/or fructose). This result is  
345 according to NMR measurements.



346

347 Figure 6: Evolution of the signal of DP 1, 3 and 4 by mass spectrometry as a function of plasma treatment  
 348 time. Oligosaccharides are detected as sodium adducts. The percentage of DP 1 was determined using  
 349 equation 1. The DP2 is not represented for esthetic reason, due to the presence of numerous matrix peaks  
 350 in the same region.

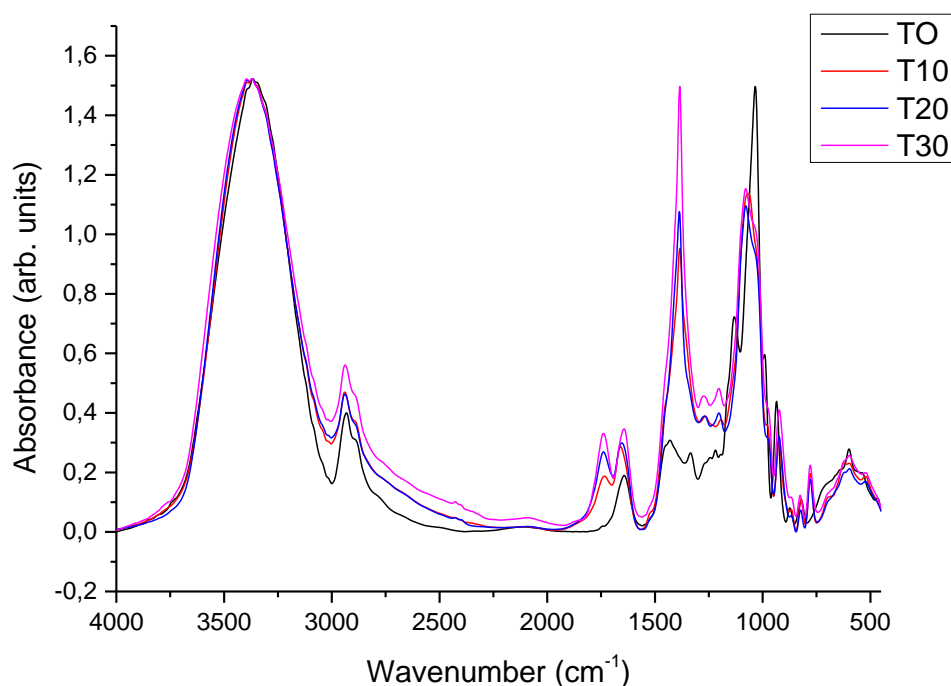
351

352 While fructose and glucose both crystallize as cyclic forms, in solution the free sugars show an  
 353 equilibrium with an acyclic form in small amount, the formation of which creates a carbonyl  
 354 group (Levy & Fügedi, 2005). This carbonyl group can react with hydroxyl groups restructuring  
 355 the hemiacetal cyclic form. For six carbon carbohydrates, like glucose and fructose, the ring  
 356 closing reaction can occur with more than one hydroxyl group, leading to isomerization and  
 357 multiple cyclic forms. Inulin is relatively chemically inert, although cleavage of the polymer  
 358 chain at any of the glycosidic bonds will produce a reactive reducing end, prone to further  
 359 reaction (Stevens, Meriggi & Booten, 2001; Wack & Blaschek, 2006).

360 2.4. Infrared bands attribution

361

362 Infrared analysis was used routinely for the assessment of chemical structure of treated inulin.  
363 The full IR description of raw inulin has been described elsewhere (Grube, Bekers, Upite &  
364 Kaminska, 2002; Ibrahim, Alaam, El-Haes, Jalbout & de Leon, 2006; Wack & Blaschek, 2006),  
365 and can be used as reference. In the first region, between 4000-2000  $\text{cm}^{-1}$ , the large broad band  
366 at 3300  $\text{cm}^{-1}$ , corresponding to the stretching of OH groups, did not change during the plasma  
367 treatment (Figure 7). A sharp band of middle intensity was noticeable at 2930  $\text{cm}^{-1}$ , assigned to  
368 the valence vibration of C-H asymmetric stretching of  $\text{CH}_2$  and a shoulder at 2890  $\text{cm}^{-1}$   
369 attributed to C-H symmetric stretching of  $\text{CH}_2$ . A deviation of the baseline with treatment time,  
370 giving rise to a broad absorption between 2400 - 3000  $\text{cm}^{-1}$  was attributed to the formation of  
371 carboxylic acids, under their dimeric form (Bellamy, 1962).



372

373 Figure 7: Infrared spectra of inulin as a function of plasma treatment time

374 In the following region, between 2000 and 1100  $\text{cm}^{-1}$ , multiple modifications were observed.  
375 Plasma treated samples showed the formation of a new band at 1740  $\text{cm}^{-1}$ , corresponding to  
376 stretching vibrations of C=O group. The band at 1640  $\text{cm}^{-1}$ , based on the existing literature

377 (Higgins, Stewart & Harrington, 1961), was assigned to adsorbed water. The light shift of the  
378 band to  $1660\text{ cm}^{-1}$  was attributed to a change of the electronic environment due to intermediate  
379 states generated during the oxidation steps, i.e. C=O formation. The bands at  $1430$  and  $1334$   
380  $\text{cm}^{-1}$  of the raw inulin are no longer visible after plasma treatment, hidden by the intensive broad  
381 band at  $1385\text{ cm}^{-1}$ , corresponding to adsorbed nitrate ion (Elmelouky, Mortadi, Chahid &  
382 Elmoznine, 2018). From T10 to T30, the presence of two bands at  $1280\text{ cm}^{-1}$  and at  $1205\text{ cm}^{-1}$   
383 indicate a structure modification from the polymer to the monomer as these bands are related  
384 to OCH and CCH bending vibrations bands of fructose and glucose. A complete disappearance  
385 of the  $1130\text{ cm}^{-1}$  band indicates the loss of C-O-C bridge character.

386 In the third region  $1100\text{-}500\text{ cm}^{-1}$ , also known as the fingerprint region, modifications are also  
387 visible. Firstly, the band at  $1030\text{ cm}^{-1}$  is reduced and hidden by a band at  $1080\text{ cm}^{-1}$  (D-fructose).  
388 All the bands ( $1035, 990, 935, 872$  and  $820\text{ cm}^{-1}$ ) related to the fructose/glucose ring structure  
389 (C-O-C ring group and ring vibrations) shift slightly towards lower values but are still present,  
390 indicating that the integrality of the monomer ring was not affected during the  
391 depolymerization. Finally, a new band is formed at  $778\text{ cm}^{-1}$  corresponding to CCO and CCH  
392 bending of D-fructose and D-glucose. From these data, inulin is depolymerized without  
393 degradation of the fructose and glucose rings. First, an oxidation of C-OH groups into  
394 carboxylic acids takes place. As the plasma treatment time increases, breakage of the C-O-C  
395 bridge of the polymer is observed.

396 It has been established in the literature (Bruggeman & Leys, 2009; Gorbanev, O'Connell &  
397 Chechik, 2016; Nastase, Tatibouët & Fourré, 2018; Shainsky, 2012), that various types of  
398 plasma-chemical species and reactions are initiated in air plasma in and in contact with liquids.  
399 Among the chemical species produced by plasma at the gas-liquid interface,  $\text{OH}^\bullet$  radical,  
400 atomic oxygen, ozone and hydrogen peroxide are the main reactive oxygen species generally  
401 accepted (Lukes, Dolezalova, Sisrova & Clupek, 2014; Sunka, 1999) to play the dominant role

402 in the reactivity. As for the nitrogen based species, nitric oxide and its derivatives formed with  
403 water (nitrites, nitrates and peroxyxynitrites) are to be considered. For example, the dissolution of  
404 the nitrous oxide gas generated in air plasma (Machala, 2013) leads to the formation of nitric  
405 and nitrous acids. The most likely reaction pathway for the depolymerization would be via the  
406 hydrolysis of the C-O-C bridge from  $H^+$  ions of  $HNO_3$  arising from the  $NO_x$  dissolution in the  
407 liquid. The slight depolymerization observed in nitrogen free plasmas could be attributed to OH  
408 radicals attack of the glycosidic bond. However, this does not explain the decrease of pH after  
409 a plasma treatment without nitrogen. Hydrogen peroxide concentration is too low to induce  
410 such pH decrease. Literature reports the formation of acids (Machala, 2013; Shainsky, 2012),  
411 arising from superoxide ion,  $O_2^-$ , that participate in the decrease of pH under nitrogen free  
412 plasma discharge and could explain our observation.

### 413 Conclusions

414 The use of renewable polysaccharide feedstocks to produce chemicals is stimulating a revival  
415 in carbohydrate chemistry employing green and sustainable processes. In this study, a new  
416 reactor has been successfully designed for the treatment of solutions or suspensions in a double  
417 dielectric barrier discharge plasma reactor. This specific reactor configuration was used in the  
418 depolymerization reaction of inulin. The conversion was strongly dependent on the gas  
419 chemical nature and reactor configuration. Pure gases of helium, nitrogen and oxygen had little  
420 effect on the depolymerization. However, plasma treatment under air led to a complete  
421 depolymerization into fructose, glucose and a DP2 compound. It appears that reactivity is at  
422 play at the gas-liquid interface, where electrons and gas species can be solvated and either attack  
423 glycosidic bonds of inulin or recombine into more reactive species. Hydrogen peroxide, nitrous  
424 and nitric oxides were identified. It appeared that the breakage of the glycosidic bond is  
425 achieved by nitric acid hydrolysis under an air plasma discharge, while OH radicals attack  
426 seems to be responsible of the small depolymerization under nitrogen free plasma. There is no

427 doubt with these results that the modification of biomass by non-thermal plasma in liquid media  
428 represents a new and non-toxic approach that would reconsider the traditional ways.

#### 429 Acknowledgements

430 The authors would like to thank the financial supports which are ADEME, Pays de Loire Region  
431 and the FR CNRS INCREASE 3707 consortium. The mass spectrometry and NMR analyses  
432 were performed using the equipment of the BIBS facility in Nantes (UR1268 BIA, IBiSA,  
433 Phenome-Emphasis-FR (grant number ANR-11-INBS-0012)).

#### 434 References

- 435
- 436 Baig, RB., & Varma, RS. (2012) Alternative energy input: mechanochemical, microwave and  
437 ultrasound-assisted organic synthesis, *Chemical Society Review*, *41*,1559-84
- 438 Bellamy, LJ. (1962) *The infra-red spectra of complex molecules*, Ed. Methuen & Co LTD.
- 439 Benoit, M., Rodrigues, A., De Oliveira Vigier, K., Fourré, E., Barrault, J., Tatibouët J.-M., &  
440 Jérôme, F. (2012) Combination of ball-milling and non-thermal atmospheric plasma as physical  
441 treatments for the saccharification of microcrystalline cellulose, *Green Chemistry*, *14*, 2212-  
442 2215
- 443 Benoit, M., Rodrigues, A., Zhang, Q., Fourré, E., De Oliveira Vigier, K., Tatibouët, J.-M., &  
444 Jérôme, F. (2011) Depolymerization of cellulose assisted by a non-thermal atmospheric plasma,  
445 *Angewandte Chemie International Edition*, *50*, 8964 –8967
- 446 Blecker, C., Fougnyes, C., Van Herck, J-C., Chevalier J-P., & Paquot, M. (2002) Kinetic study  
447 of the acid hydrolysis of various oligofructose samples, *Journal of Agricultural Food*  
448 *Chemistry*, *50*, 1602-1607
- 449 Bruggeman, PJ., Kushner, MJ., Locke, BR., Gardeniers, JGE., Graham, WG., Graves, DB.,  
450 Hofman-Caris, RCHM., Maric, D., Reid, JP., Ceriani, E., Fernandez Rivas, D., Foster, JE.,

451 Garrick, SC., Gorbanev, Y., Hamaguchi, S., Iza, F., Jablonowski, H., Klimova, E., Kolb, J.,  
452 Krcma, F., Lukes, P., Machala, Z., Marinov, I., Mariotti, D., Mededovic Thagard, S., Minakata,  
453 D., Neyts, EC., Pawlat, J., Lj Petrovic, Z., Pflieger, R., Reuter, S., Schram, DC., Schröter, S.,  
454 Shiraiwa, M., Tarabová, B., Tsai, PA., Verlet, JRR., von Woedtke, T., Wilson, KR., Yasui, K.,  
455 & Zvereva, G. (2016) Plasma–liquid interactions: a review and roadmap, *Plasma Sources*  
456 *Science and Technologies*, 25, 053002

457 Bruggeman, P., & Leys, C. (2009) Non-thermal plasmas in and in contact with liquids, *Journal*  
458 *of Physics D: Applied. Physics*, 42, 053001

459 Colombo, C., Aupic, C., Lewis, A.R., & Mario Pinto, B. (2015) In situ determination of fructose  
460 isomer concentrations in wine using <sup>13</sup>C quantitative nuclear magnetic resonance spectroscopy,  
461 *Journal of Agriculture and food chemistry*, 63, 8551 - 8559

462 Elmelouky, A. Mortadi, A., Chahid, El., Elmoznine, R. (2018) Impedance spectroscopy as a  
463 tool to monitor the adsorption and removal of nitrate ions from aqueous solution using zinc  
464 aluminum chloride anionic clay, *Heliyon*, 4, e00536

465 Farmer, JT., & Mascal, M. (2015). Platform molecules. In Clark, J., Deswarte, & F.,  
466 *Introduction to chemicals from biomass*, 2<sup>nd</sup> Edition (pp.89-156). John Wiley & Sons, Ltd.

467 Gorbanev, Y., O’Connell, D., & Chechik, V. (2016) Non thermal plasma in contact with water:  
468 the origin of species, *Chemistry: a European Journal*, 22, 3496-3505

469 Grube, M., Bekers, M., Upite, D., & Kaminska, E. (2002) E. Infrared spectra of some fructans,  
470 *Spectroscopy*, 16, 289-296

471 Higgins, HG., Stewart, CM., & Harrington, KJ. (1961) Infrared spectra of cellulose and related  
472 polysaccharides, *Journal of polymer chemistry*, 51,59-84

473 Horváth, HT., & Anastas, PT. (2007) Innovations and green chemistry, *Chemical Reviews*, 107,  
474 2169-2173

475 Ibrahim, M., Alaam, M., El-Haes, H., Jalbout, AF., & de Leon, (2006) F. Analysis of the  
476 structure and vibrational spectra of glucose and fructose, *Ecletica Quimica*, 31, 15-21

477 Jérôme, F. (2016) Non-thermal atmospheric plasma: opportunities for the synthesis of valuable  
478 oligosaccharides from biomass, *Current Opinion in Green and Sustainable Chemistry*, 2, 10-  
479 14

480 Jérôme, F., Chatel G., & De Oliveira Vigier, K. (2016) Depolymerization of cellulose to  
481 processable glucans by non-thermal technologies, *Green Chemistry*, 18, 3903-3913

482 Kan, CW., Lam, CF., Chan, CK., & Ng, SP. (2014) Using atmospheric pressure plasma  
483 treatment for treating grey cotton fabric, *Carbohydrate Polymers*, 15, 167-73

484 Levy DE., & Fügedi, P. (2005) *The Organic Chemistry of Sugars*, CRC Press and Taylor and  
485 Francis Group

486 Lukes, P., Dolezalova, E., Sisrova, I., & Clupek, M. (2014) Aqueous-phase chemistry and  
487 bactericidal effects from an air discharge plasma in contact with water, *Plasma Sources Science  
488 and Technologies.*, 23, 015019

489 Machala, Z., Tarabova, B., Hensel, K., Spetlikova, E., Sikurova, L., & Lukes, P. (2013)  
490 Formation of ROS and RNS in water electro-sprayed through transient spark discharge in air  
491 and their bactericidal effects, *Plasma Process and Polymers*, 10, 649-659

492 Mariotti, D., Patel, P., Švrček, V., & Maguire, P. (2012) Plasma-liquid interactions at  
493 atmospheric pressure for nanomaterials synthesis and surface Engineering, *Plasma Process.  
494 Polym*, 9, 1074-1085



495 Nastase, R., Tatibouët, J-M., & Fourré, E. (2018) Depolymerization of inulin in the highly  
496 reactive gas phase of a non-thermal plasma at atmospheric pressure. *Plasma Process and*  
497 *Polymers*, 15, 1800067

498 National Research Council. *Plasma processing of materials: scientific opportunities and*  
499 *technological challenges*. (1991) Washington, DC: The National Academies Press

500 Ong, HC., Chen, WH., Farooq, A., Gan, YY., Lee, KT., & Ashokkumar, V. (2019) Catalytic  
501 thermochemical conversion of biomass for biofuel production: a comprehensive review,  
502 *Renewable & Sustainable Energy Reviews*, 113, 109266

503 Pankaj, SK., & Keener, KM. (2017) Cold plasma: background, applications and current trends.  
504 *Current Opinion in Food Science*, 16, 49–52

505 Postek, MT., Moon, RJ., Rudie, AW., & Bilodeau, MA. (2013) *Production and Applications*  
506 *of Cellulose Nanomaterials*, Tappi Press

507 Raccuia, SA., Genovese, G., Leonardi, C., Bognanni, R., Platania, C., Calderaro P., & Melilli,  
508 MC. (2016) Fructose production by *Cynara cardunculus* inulin hydrolysis, *Acta Horticulturae*,  
509 43, 309-314

510 Ropartz, D., Bodet, P-E., Przybylski, C., Gonnet, F., Daniel, R., Fer, M., Helbert, W., Bertrand,  
511 D., & Rogniaux, H. (2011) *Rapid Communication in Mass Spectrometry*, 25, 2059–2070

512 Shainsky, N., Dobrynin, D., Ercan, U., Joshi, SG., Ji, H., Brooks, A., Fridman, G., Cho, Y.,  
513 Fridman, A., & Friedman, G. (2012) Plasma acid: water treated by dielectric barrier discharge,  
514 *Plasma Process and Polymers*, 10, 1-6

515 Sheldon, RA. (2018) Chemicals from renewable biomass: a renaissance in carbohydrate  
516 chemistry, *Current Opinion in Green and Sustainable Chemistry*, 14, 89-95

517 Shiomi, N., & Onodera, S. (1990) The  $^{13}\text{C}$ -NMR spectra of inulo-oligosaccharides,  
518 *Agricultural Biological Chemistry.*, *54*, 215–216

519 Stevens, CV., Meriggi, A., & Booten, K. (2001) Chemical modification of inulin, a valuable  
520 renewable resource, and its industrial applications, *Biomacromolecules*, *2*, 1-16

521 Sunka, P., Babicky, V., Lupek, MC., Lukes, P., Simek, M., Schmidt, J., & Cernak, M. (1999)  
522 Generation of chemically active species by electrical discharge in water, *Plasma Sources*  
523 *Science and Technology*, *8*, 258–265

524 Sylla-Iyarreta Veitía, S., & Ferroud, C. (2015) New activation methods used in green chemistry  
525 for the synthesis of high added value molecules, *International Journal of Energy and*  
526 *Environmental Engineering.*, *6*, 37-46

527 Takai, O. (2008) Solution plasma processing (SPP), *Pure and Applied Chemistry*, *80*, 2003-  
528 2011

529 Tarabova, B., Lukes, P., Janda, M., Hensel, K., Sikurova, L., & Machala, Z. (2018) Specificity  
530 of detection methods of nitrites and ozone in aqueous solutions activated by air plasma, *Plasma*  
531 *Process and Polymers*, *15*, 1800030

532 Tendero, C., Tixier, C., Tristant, P., Desmaison, J., & Leprince, P. (2006) Atmospheric pressure  
533 plasmas: a review, *Spectrochimica. Acta Part B*, *61*, 2-30

534 Wack, M., & Blaschek, W. (2006) Determination of the Structure and Degree of Polymerisation  
535 of Fructans from Echinacea Purpurea Roots, *Carbohydrate Research*, *341*, 1147-53